Structure of the Membrane Binding Domain of CTP:Phosphocholine Cytidylyltransferase[†,‡]

Simon J. Dunne,[§] Rosemary B. Cornell,* Joanne E. Johnson, Nicholas R. Glover, and Alan S. Tracey

Department of Chemistry and Institute of Molecular Biology and Biochemistry, Simon Fraser University, Burnaby, BC, Canada V5A 1S6

Received April 5, 1996; Revised Manuscript Received July 9, 1996[⊗]

ABSTRACT: It has been proposed that the domain of the regulatory enzyme, CTP:phosphocholine cytidylyltransferase, which mediates reversible binding of the enzyme to membranes, is an amphipathic α-helix of approximately 60 amino acid residues and that this domain is adjacent to the putative active site domain of this enzyme. Circular dichroism indicated that the secondary structures of two overlapping peptides spanning this region were predominantly α-helical in the presence of PG vesicles or sodium dodecyl sulfate micelles. Interproton distances were obtained from two-dimensional NMR spectroscopic measurements to solve the structures of these two peptides. The C-terminal 22 amino acid peptide segment (corresponding to Val267−Ser288) was a well-defined α-helix over its length. The N-terminal 33-mer (corresponding to Asn236−Glu268) was composed of an α-helix from Glu243 to Lys266, a well-structured bend of about 50° at Tyr240−His241−Leu242, and an N-terminal four-residue helix. It is proposed that the three residues involved in generating the bend act as the hinge between the catalytic and regulatory domains. The nonpolar faces of the 33-mer and 22-mer were interrupted by Ser260, Ser271, and Ser282. These residues may serve to limit the hydrophobicity and facilitate reversible and lipid-selective membrane binding. The hydrophobic faces of the helices were flanked by a set of basic amino acid residues on one side and basic amino acid residues interspersed with glutamates on the other. The disposition of these side chains gives clues to the basis for the specificities of these peptides for anionic surfaces.

CTP:phosphocholine cytidylyltransferase (CT)[1] is a regulatory enzyme in the synthesis of phosphatidylcholine (PC), the major phospholipid of animal cells. The membrane PC content is tightly regulated so that there is little alteration in responses to changes in the metabolic state of the cell. Agonists that stimulate PC turnover also stimulate the synthesis of PC. In many instances, the regulation is directed at CT (Tronchere et al., 1994). The principal mode for regulation of CT is via an interconversion between the membrane (active) and cytoplasmic (inactive) forms (Tronchere et al., 1994). Two classes of membrane lipids (anionic lipids and diacylglycerol) stabilize the membrane-bound form, whereas phosphorylation of the transferase stabilizes the inactive form. Surprisingly, CT is a nuclear enzyme (Wang et al., 1993, 1995), but the role of its nuclear localization is not yet clear.

Amphitropism (Burn, 1988) is a feature CT shares with many metabolic enzymes. Examples include phosphatidic acid phosphatase, diacylglycerol kinase, phospholipase A2, and a number of other proteins important in transducing extracellular signals such as raf, guanine nucleotide exchange proteins, G proteins, src-type kinases, and protein kinase C. In some cases, membrane binding is mediated by reversible lipid covalent anchoring (Casey, 1995) while, in other cases, protein motifs such as zinc butterflies (Zhang et al., 1995), C_2 domains (Sutton et al., 1995), or Pleckstrin homology domains (Timm et al., 1994) are the likely mediators. The precise chemistries involved in these lipid−protein interactions are only just beginning to be understood.

There is abundant evidence that the membrane interaction of CT is mediated by an amphipathic α-helix between residues 235 and 298 (domain M). Domain M constitutes a discrete exon in the mouse CT gene (Rutherford et al., 1993), and its sequence is highly conserved with only two nonconservative changes among five sequenced mammalian CTs (Sweitzer & Kent, 1994; Kalmar et al., 1994; Hogan et al., 1995). It contains an 11-mer motif repeated three times in tandem between amino acids 256 and 288. Removal of domain M, using proteolysis (Craig et al., 1994) or cDNA mutation (Cornell et al., 1995; Wang & Kent, 1995; Yang et al., 1995), resulted in loss of membrane association both *in vitro* and *in vivo.* The structure of peptides corresponding to portions or all of domain M have been studied by circular dichroism (CD). The peptides were predominently random coil in the absence of lipid vesicles and α-helical in the presence of anionic lipid vesicles (Johnson & Cornell, 1994; Johnson, 1995). Quenching of the tryptophan fluorescence with brominated phospholipid derivatives suggested that the peptides intercalate halfway into the outer monolayer of the lipid vesicles (Johnson & Cornell, 1994). In addition to the evidence from peptide analysis, direct photolabeling of intact

[†]This work was supported by grants from the Natural Sciences and Engineering Research Council of Canada (A.S.T.) and the Medical Research Council of Canada (R.B.C. and a studentship to J.E.J.).

[‡] The structure information has been deposited with the Brookhaven Protein Data Bank under the filenames 1PEH, 1PEI, R1PEHMR, and R1PEIMR.

* Corresponding author.

[§] Present address: Institut fur Anorganishe Chemie, Universitat Basel, CH-4056 Basel, Switzerland.

[⊗] Abstract published in *Advance ACS Abstracts,* September 1, 1996.

[1] Abbreviations: CT, CTP:phosphocholine cytidylyltransferase; SDS, sodium dodecyl sulfate; PC, phosphatidylcholine; DPC, dodecylphosphocholine; PG, phosphatidylglycerol; CD, circular dichroism; NOE, nuclear Overhauser effect; COSY, correlation spectroscopy; DQF-COSY, double quantum filtered COSY; TOCSY, total correlation spectroscopy; NOESY, nuclear Overhauser effect spectroscopy.

S0006-2960(96)00821-5 CCC: $12.00

CT with the hydrophobic probe 3-(trifluoromethyl)-3-(*m*-[^{125}I]iodophenyl)diazirine ([^{125}I]TID), implicated domain M as the principal domain mediating membrane intercalation (Johnson, Aebersold, and Cornell, unpublished). TID, when incorporated into anionic lipid vesicles, labeled an 8 kDa domain which was identified as domain M by sequencing (Johnson, Aebersold, and Cornell, unpublished).

These data suggest that domain M of CT orients with its helical axis parallel to the membrane surface such that the hydrophobic face of the amphipathic helix intercalates into the lipid core. The N- and C-terminal domains flanking the amphipathic helix would then project into the aqueous phase via appropriately situated bends.

One model for the activation of CT proposes that domain M is autoinhibitory because of an interaction of M with the active site that interferes with substrate binding or turnover. When domain M is bound to lipid, the inhibition is relieved (Wang & Kent, 1995). The evidence for this model is the constitutive activity of a CT mutant lacking all of domain M (Wang & Kent, 1995). The basic secondary structure of domain M of CT may be the same in the presence or absence of lipids, due to stabilization of the α-helix by interactions with the catalytic domain in the absence of lipids. The key conformational change might then be a movement of the amphipathic helix, mediated by a flexible hinge between the catalytic and membrane binding domains.

All previous structural studies of the membrane binding domain have relied on low-resolution and/or indirect methods. Here we present the highly resolved NMR-derived structures of two overlapping peptides bound to SDS. These 33-mer and 22-mer peptides encompass nearly all of domain M. Attempts to solve the structure of a 62-mer peptide corresponding to the entire domain M were unsuccessful due to incomplete spectral resolution. However, all the spectral information obtained for the 62-mer was compatible with the solved structures of the N-terminal and C-terminal component peptides. The results show conclusively that, in the presence of amphiphiles, the membrane binding domain of CT is an amphipathic α-helix that is linked via a turn to the N-terminal domain of the enzyme. Furthermore, the arrangement of side chains in the helix sheds light on questions concerning the lipid specificity for binding, helix stability, and the driving force for membrane binding.

MATERIALS AND METHODS

Materials. All peptides were provided by Ian Clark-Lewis (University of British Columbia) (Clark-Lewis et al., 1991). After HPLC and lyophilization the peptides were 99% pure and essentially salt free. The 22-mer (PEPC22) corresponds to residues 267−288 of rat liver CT, and the 33-mer (PEPNH1) spans the region 236−268, while PEP62 overlaps these, extending from residue 238 to residue 299. The numbering throughout corresponds to that of the native sequence of rat liver CT (Kalmar et al., 1990). In order to facilitate fluorescence studies (Johnson, 1995), phenylalanine-263 of the native sequence was replaced by a tryptophan in PEPNH1. The peptides were acetylated at the N-terminal position and aminated at the C-terminal position in order to eliminate the influence of charged groups at the terminal positions. Perdeuterated sodium dodecyl sulfate (SDS-d_{25}) was purchased from Cambridge Isotope Laboratories Inc., and D_2O was obtained from STOHLER/KOR Stable Isotopes Inc. Dioleoylphosphatidylglycerol (PG) was purchased from Avanti Polar Lipids. Insight II (version 2.3) and Felix (version 2.1, Hare Research Inc.) software were purchased from Biosym Technologies Ltd.

CD Measurements. Samples were prepared by mixing aqueous solutions of peptide with aqueous SDS micelles or phospholipid vesicles. The pH of the samples was ∼5.0. The peptide concentration was 100 μM and the amphiphile/peptide ratio was 40:1. Dioleoyl-PG vesicles were prepared as previously described (Johnson & Cornell, 1994). CD spectra were obtained at 25 °C using a JASCO 700 spectropolarimeter using the techniques previously reported (Johnson & Cornell, 1994). The percent helix content was estimated from θ_{222} values (Chang et al., 1978).

NMR Sample Preparation. The CT peptides (3.7 μmol of PEPC22, 1.2 μmol of PEPNH1, and 2.8 μmol of PEP62) were dissolved in 0.75 mL of 90% H_2O/10% D_2O, together with an appropriate amount of SDS-d_{25} to give a lipid to peptide molar ratio of 40:1, for PEPC22 and PEPNH1, and 80:1, for PEP62. The pH was then adjusted with aliquots of 0.1 M NaOD to values that gave sufficiently resolved amide signals in the NMR spectrum: pH 5.20 for PEPC22, pH 6.02 for PEPNH1, and pH 6.08 for PEP62.

NMR Methods. All spectra were obtained using a Bruker AMX600 spectrometer operating at 600.13 MHz. All two-dimensional spectra used for the structural analysis were recorded at 298 K in the phase-sensitive mode using time-proportional phase incrementation (TPPI). A recycle delay of 1.5 s and a spectral width of 8124 Hz were employed to collect 512 t_1 increments with 32 transients in 2048 data points. For the TOCSY and NOESY experiments, the ^1H_2O signal was suppressed using the pulsed field gradient "WATERGATE" technique (Piotto et al., 1992) incorporating a 3−9−19 pulse sequence (Sklenar et al., 1993). For the DQF-COSY experiments (Rance et al., 1983) the water signal was suppressed using a 2 s presaturation pulse during the recycle delay. The TOCSY spectra were recorded using the MLEV-17 mixing sequence with 2.5 ms trim pulses before and after mixing. The MLEV-17 spin-lock pulse was applied for 75 and 150 ms at a 17.9 kHz power level. A series of NOESY spectra, covering the range 50−200 ms, were recorded using a standard pulse sequence with water suppression.

The NMR spectra were processed using the UXNMR package (Bruker) on an Aspect X32 workstation and also the FELIX program on an Indigo2 computer (Silicon Graphics Inc.). Prior to Fourier transformation, the data were zero-filled to generate a 2K × 2K two-dimensional matrix and apodized by a quadratic sine-bell window function in both dimensions. Automatic base-line corrections with a fourth-order polynomial function were applied, in both dimensions, to all processed spectra. All chemical shifts were referenced to the methyl resonance of 4,4-dimethyl-4-silapentane-1-sulfonate (DSS) as an external standard at 298 K.

NMR-Derived Constraints. Nuclear Overhauser effect enhancement (NOE) distance constraints for molecular modeling were obtained from NOESY data by measuring cross-eak volumes within the FELIX program. Visual cross-checking was necessary to ensure that partial signal overlap did not skew integrated cross-peak volumes. Adjustments were made as necessary. The NOE constraints were then put into three overlapping classes: strong (1.8−3.0 Å), medium (2.7−4.0 Å), and weak (3.8−5.0 Å). Intraresidue $H_{\beta\beta}$ cross-peaks were used as internal distance standards

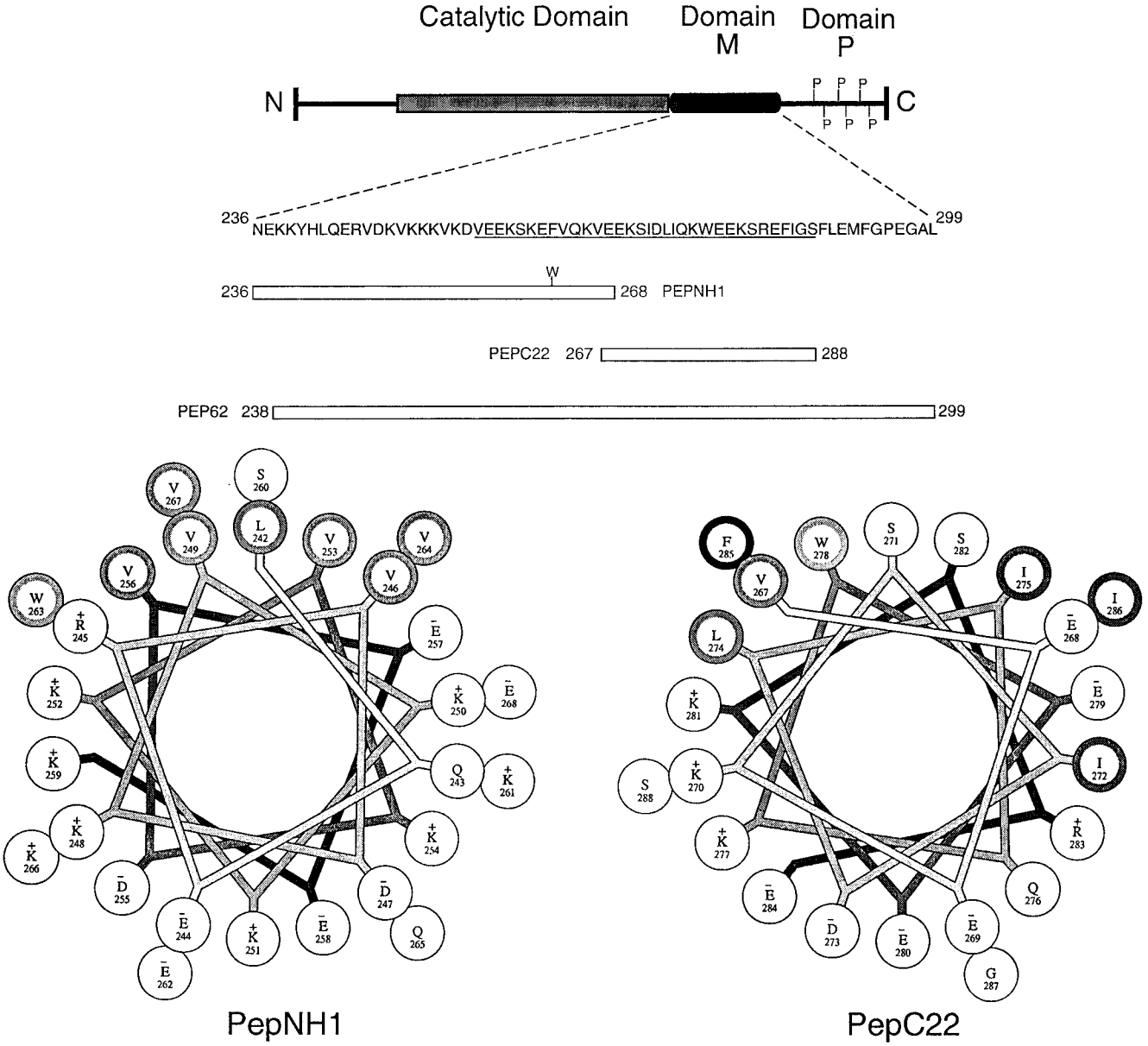

FIGURE 1: (A) Domain structure of CT: sequence of domain M and diagrams of the peptides used in this study. (B, bottom) Helical wheel plots of PEPC22 (right) and residues 242−268 of PEPNH1 (left). Hydrophobic side chains are indicated by shaded outlines.

(1.75 Å). Most NOE enhancements were observed for both 100 and 200 ms mixing times. Weak enhancements (only prominent at 200 ms mixing times) were included in the restraint set only if spin diffusion effects could be eliminated by inspection of the NOE enhancement buildup curves. In total, 442 restraints (253 intraresidue and 189 interresidue) were used for modeling the PEPNH1 structure and 286 restraints (151 intraresidue and 135 interresidue) for the PEPC22 structure.

Distance Geometry and Simulated Annealing Calculations. All calculations and graphic visualizations were performed on an Indigo2 workstation (Silicon Graphics Inc.) using the program INSIGHT II (Biosym Technologies). Using the above described constraints, the distance geometry/simulated annealing (DG/SA) protocol was applied by the INSIGHT II program. Ten initial structures were generated using metric matrix distance geometry techniques at the smoothing and embedding stages of the DGII module. Before the structures were "annealed", the initial energy was previewed and suitable values were found to be 1450 kJ/mol (PEPNH1) and 1000 kJ/mol (PEPC22). The fail level was set so that the SA routine was forced to calculate the mirror image and not proceed to the energy minimization routine. A tighter ensemble of structures was generated when the calculations were halted at this stage. Energy minimization is complicated by the peptide-amphiphile interactions which are not accounted for in the SA calculations. For each peptide, all ten calculated structures were very similar.

RESULTS

Three peptides of the cytidylyltransferase lipid binding domain were examined in this study. PEP62 corresponds to residues 238−299 of rat liver CT (Kalmar et al., 1990) and spans the complete binding region. PEPNH1 corresponds to the N-terminal segment of the 62-mer (residues 236−268) and is substituted at Phe263 of the native sequence with a tryptophan. The third peptide, PEPC22, corresponds to residues 267−288. The amino acid sequences and helical wheel plots of PEPC22 and PEPNH1 are shown in Figure 1.

Circular Dichroism Studies of CT Peptides Bound to Sodium Dodecyl Sulfate Micelles and to Lipid Vesicles. In water, the CD spectra of the CT peptides were indicative of

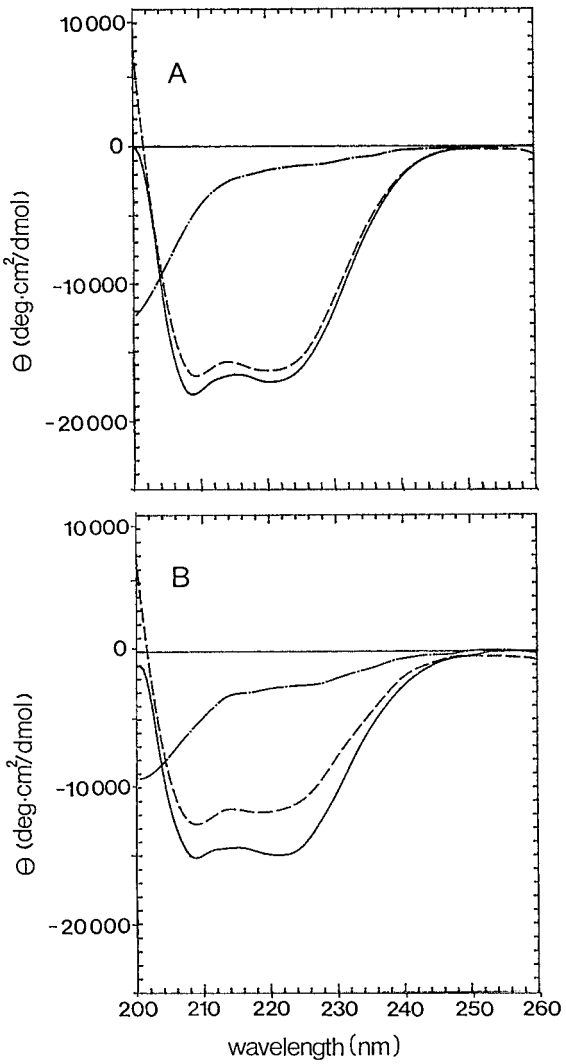

FIGURE 2: CD spectra of PEPNH1 (A) and PEPC22 (B) in water (· — ·), 4 mM sodium dodecyl sulfate (— —), and 4 mM dioleoylphosphatidylglycerol (—). Peptide concentration = 100 μM.

predominently random coil conformation (Figure 2). The CD spectra did not change upon addition of up to 4 mM zwitterionic amphiphile dodecylphosphocholine (data not shown). However, in the presence of anionic amphiphiles such as SDS they adopted a predominently α-helical structure (Figure 2). The CD spectra of PEPNH1 were similar when obtained in the presence of either SDS or PG vesicles (Figure 2A) and indicated that the peptides adopted conformations that were primarily α-helical (in SDS, 49%; in PG, 51%). The CD spectra for PEPC22 in the presence of either of the amphiphiles were also similar but did suggest a slightly higher α-helical content when in the presence of PG compared to SDS (Figure 1B; 41% in SDS; 50% in PG). The percent helicity values obtained from CD data provide crude estimates but are useful for comparison. It is evident from the CD spectra that these peptides have the same conformational preference when bound to an SDS micelle as when bound to a lipid bilayer vesicle.

Proton NMR Assignments. In the absence of added SDS, the proton NMR spectra of the peptides were well resolved, and no significantly intense cross-peaks were measured in the NOESY spectra. This indicated that the peptides had no preferred conformation but rather existed in a random coil arrangement. This is in agreement with the CD spectra which also suggested the peptides were unstructured in water. To obtain the structures of the peptides in their amphiphile-

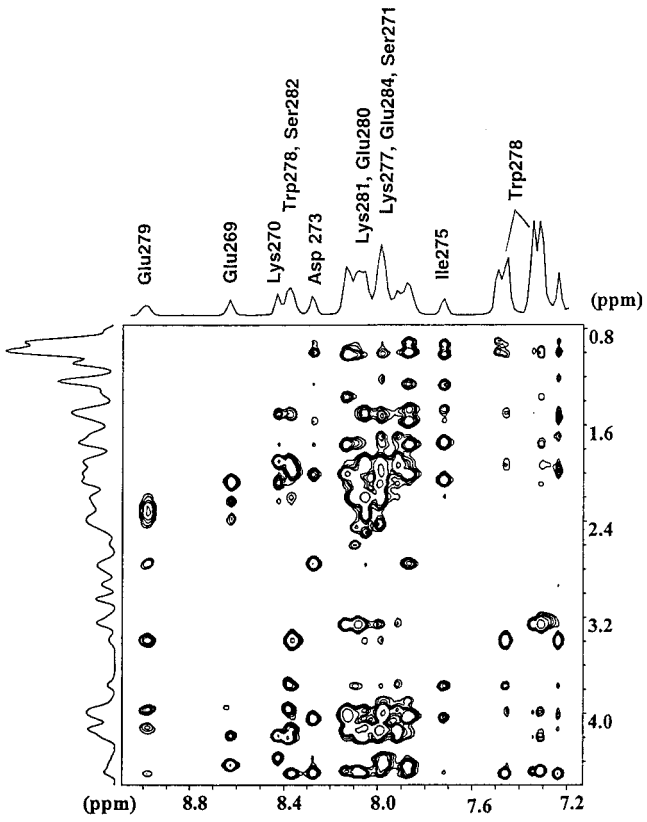

FIGURE 3: Partial 2D NOESY spectrum from PEPC22 showing the fingerprint region together with some of the aromatic cross-peak region and the corresponding portions of the 1D spectra. Only some of the NH signals are labeled. The 2D spectrum was obtained at 298 K using a 200 ms mixing time for the buildup of the NOE cross-peak signals.

bound conformations, NMR spectra were acquired in the presence of SDS micelles. Unlike peptide/vesicle complexes, the rate of tumbling of peptide−SDS micelles is fast enough to give NMR signals that are sharp enough for resolution of two-dimensional spectra. Except for a few signals, e.g., the tyrosine ring, the signals were not sharp enough for determination of *J* coupling constants, which would have aided the structure determination. Figure 3 shows a partial 2D spectrum from PEPC22 and the associated 1D spectral regions. Two regions of spectral crowding are evident, and it is also clear that measurement of *J* couplings is not possible.

Sequence-specific NMR assignments were obtained using standard procedures for small proteins (Wüthrich, 1986). Because of some sequence repeats in the two peptides and 10 lysines in PEPNH1, there was extensive overlap in some regions of the homonuclear ^{1}H spectra (see Figure 3). However, near complete proton assignments could be made for both peptides using TOCSY spectra to identify spin-coupled networks, NOESY spectra to establish interresidue contacts and to resolve degenerate spin systems, and DQF-COSY spectra to confirm intraresidue connectivities. Where spectral overlap was problematic, recourse was made to a set of spectra recorded at 310 K in which the spin connectivity networks of some residues were better resolved. The predominent remaining ambiguities in the spectra arose for some of the lysine residues of the 33-residue peptide. The degree of signal overlap for 6 of the 10 lysines (Lys-250, -251, -254, -259, -261, -266) was such that the $H_{\delta,\epsilon}$ proton signals could not be unambiguously assigned. This does suggest that these lysines are, chemically, very similar.

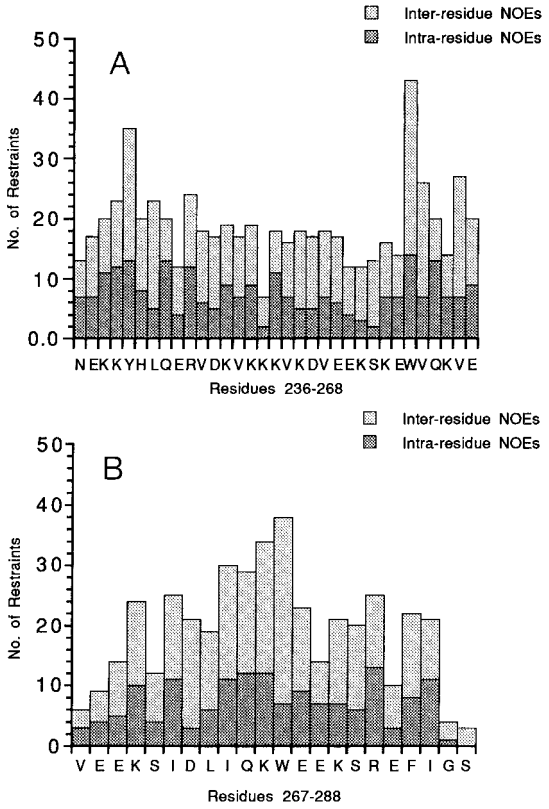

FIGURE 4: Graphical representation of the distribution of inter- and intraresidue NOE constraints for (A) PEPNH1 and (B) PEPC22.

The spectral assignments are given in Supporting Information.

Secondary Chemical Shifts Indicate an α-Helical Structure. If a peptide or protein has an ordered conformation, the chemical shift changes from that of a random coil arrangement and can be correlated with unique secondary structure elements (Wüthrich, 1986; de Dios et al., 1993; Le et al., 1995). For example, H_α resonances are found at higher field in an α-helical conformation and at lower field in a β-sheet structure (Wüthrich, 1986; Wishart & Sykes, 1991; Wishart et al., 1992). The H_α secondary shift (ΔH_α) values were indicative of an α-helical structure for both peptides. ΔH_α values are given in Supporting Information. The residues with downfield ΔH_α values in PEPC22 (Glu268, 0.15; Lys270, 0.01: and Gly287, 0.06) are located near the termini where dynamic "fraying" disrupts the helical pattern. The signals with downfield ΔH_α values in PEPNH1 (Tyr240 and His241, 0.01 and 0.19) arise from protons adjacent to aromatic rings where the ring currents could influence the spectrum. However, in this case, the calculated structure shows that the Tyr240 and His241 residues are situated in a turn rather than in an α-helix, and this probably is the source of the major contribution to a downfield ΔH_α. The other aromatic residues, all of which are found within the helical region, show negative ΔH_α secondary shifts. The average upfield shift for the H_α protons of PEPNH1, neglecting the two residues in the turn, was 0.36 ± 0.20 ppm. The average upfield shift for an α-helix is 0.35 ppm (Rizo et al., 1993). For PEPC22 the average upfield shift was 0.20 ± 0.12 ppm.

Nuclear Overhauser Effect Enhancements and Secondary Structure. In total, 442 and 286 NOE constraints were used in modeling the PEPNH1 and PEPC22 structures, respectively. The number of intra- and interresidue restraints for each amino acid in each peptide is indicated in Figure 4. Panels A and B of Figure 5 show many of the interresidue NOE connectivities for PEPNH1 and PEPC22. The medium strength *i, i*+3 connectivities are characteristic of an α-helix. Utilization of these NOE constraints in the BIOSYM Insight II molecular modeling package provided an ensemble of calculated structures. Both PEPNH1 and PEPC22 peptide backbone structures were well defined (Figure 6 A,B). The root mean square deviations of the backbone atoms, from the mean values for the ensemble of structures, were less than 0.2 Å for all but the terminal residues (Figure 7). Even in the cases where the side chain NMR spectra were well resolved, the side chains generally had much less restriction placed on their motion by the NOE constraints than did the backbone residues.

Backbone Structure. PEPNH1 had an α-helical structure from residue Leu242 to the C-terminal Glu268. The final two residues of the C-terminus did show some minor fraying from the helical structure. The distance, $C_\alpha - C_\alpha$, from Gln243 to Lys266 was 37.6 ± 0.4 Å (average of five structures). This distance would be 36 Å for a perfect α-helix. The first four N-terminal amino acid groups, Asn236 through Lys239, formed a helical arrangement (average Ψ and Φ values of −43 ± 6° and −58 ± 8)°, respectively) that was coupled to the α-helical region by a well-defined bend of about 50°. The bend occurred between Tyr240 and Leu242 (Figures 6 and 8). Figure 6 shows that the bend is the most well defined backbone region of PEPNH1. It is not an artifact arising from lack of resolved cross-peaks, since many of the best resolved signals in the 2D NMR spectra arose from the first eight residues in PEPNH1, including Tyr240 and His241 (data not shown). A total of 77 NOE contacts were obtained for the residues constituting the bend (Figure 4). Disruption of the helical structure is evident from Figure 5A. The $H_\alpha^i - H_N^{i+3}$ backbone contacts characteristic of an α-helix that were abundant for the region Gln243−Gln265 were abruptly halted at this portion of the sequence (Figure 5A). The few $H_\alpha^i - H_\beta^{i+3}$ contacts within the first four residues of PEPNH1 do not overlap with those of the helical section beginning at Leu242. Figure 8 provides a stereo diagram of the bend and flanking regions and shows the spatial orientation of the associated side chains.

PEPC22 had a well-defined α-helical structure along its entire length. Unlike PEPNH1, the *i, i*+3 NOE contacts of PEPC22 were overlapped throughout its entire sequence. The different calculated structures varied significantly from each other only at the terminal positions. Such differences may represent a less restricted motion at these positions or may simply result from less available NOE constraints for the terminal residues. The calculated structures for PEPC22 show much more disorder at the terminal positions than those for PEPNH1. The length of the peptide backbone, averaged for three structures, was 31.2 ± 0.3 Å. A perfect α-helix of 22 residues would have a length of 33 Å. The difference between the ideal and observed distances probably arises from the loss of structure at the terminal positions.

Unfortunately, the two-dimensional spectra did not provide adequate resolution of the 62-residue peptide. The two regions of major signal overlap, from 7.8 to 8.5 ppm, seen in Figure 3 for PEPC22, were similarly overlapped in PEPNH1. The superposition of these overlapped regions in the 62-mer effectively prevented analysis of the spectrum. However, all the α-proton signals detected in the spectra of PEP62 had upfield secondary shifts within the range of

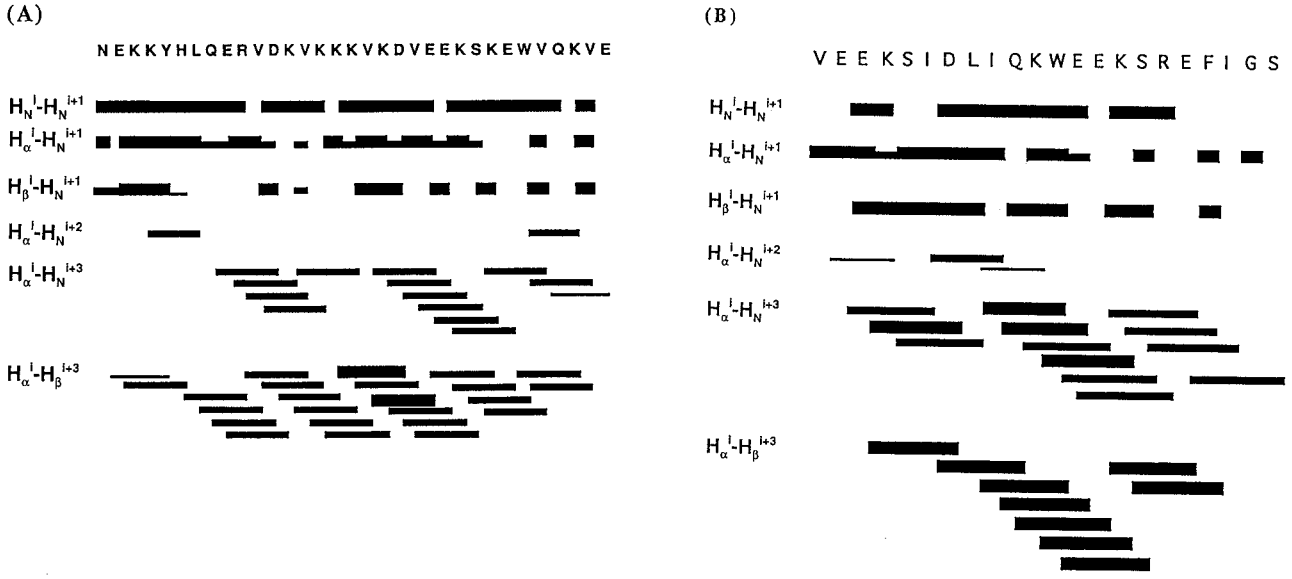

FIGURE 5: Selected interresidue NOE connectivities from the NOESY spectra of (A) PEPNH1 and (B) PEPC22. The relative strengths of the interactions are indicated by the bar widths.

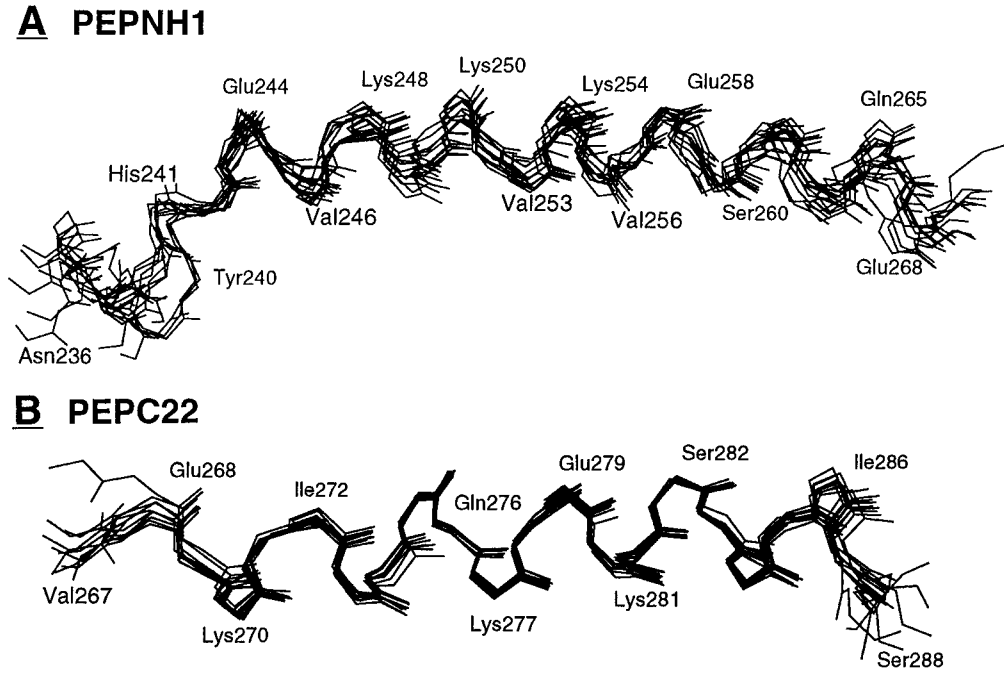

FIGURE 6: Conformational ensembles of 10 calculated structures for (A) PEPNH1 and (B) PEPC22. For these arrays, the backbone atoms for residues 238−266 (PEPNH1) and 269−286 (PEPC22) were superimposed.

chemical shifts observed for the 22- and 33-residue peptides. In addition, some of the better resolved signals in the spectrum of PEP62 formed a pattern that conformed to similar regions in the spectra of PEPNH1 and C22. These observations suggest a structure for the 62-mer that is a simple amalgamation of PEPNH1 and PEPC22 structures, with PEPC22 representing an extension of the C-terminal α-helical portion of PEPNH1.

Side Chain Conformations. The arrangement of the various side chain residues on the backbone structure leads to well-defined amphipathic helices for the α-helical region of both PEPNH1 and PEPC22. In PEPNH1, the nonpolar sector is flanked by Arg245, Lys252, Lys259, and Lys266 on one side and by Gln243, Lys250, Glu257, Lys261, and Glu268 on the other. Thus, each turn of the helix contributes a polar sidechain to alternating sides of the polar/nonpolar interface. In PEPC22 the nonpolar sector is flanked by Lys270, Lys277, and Lys281 on one side and by Glu268, Glu279, and Arg283 on the other. Notable exceptions to the segregation of polar side chains from nonpolar side chains are the positioning of Ser260 in PEPNH1 and of Ser271 and Ser282 in PEPC22 into the nonpolar face.

The conformations of the many lysine side chains were investigated. Gauche rotomers (±g) about the $\gamma-\delta$ bond were common, but frequently about one-half of the ensemble of calculated structures was all-trans and the remainder contained one or more gauche rotomers. This ambivalence may simply reflect the paucity of data for certain lysines (such as Lys251, -254, -259) where the protons of the side chain were not resolved in the NMR spectra. Gauche rotations along the lysine side chain could bring the δ and ϵ protons into closer proximity to the NH and H_α protons of the peptide backbone. This would cause a time-averaged NOE buildup in the corresponding cross-peaks. Because of the $1/r^6$ distance relationship for the NOE buildup, a disproportionate signal intensity would be obtained. For

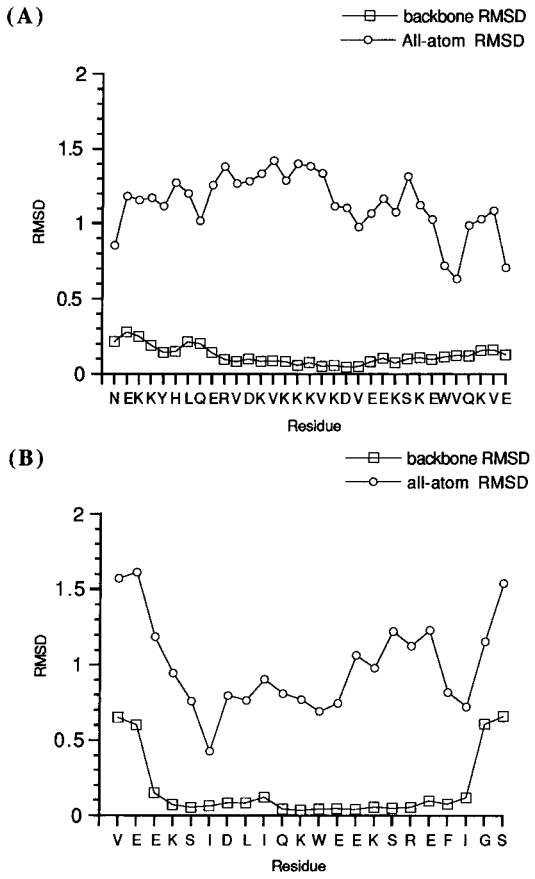

FIGURE 7: Pairwise RMSD from the mean structure shown as a function of residue position for: (A) PEPNH1 and (B) PEPC22. Backbone atoms, N−C_α−C═O, are represented by □ and all atoms by ○. The plots were generated by moving a three-residue window along the sequence and plotting the mean pairwise RMSD (Å) over the central residue. For the first and last residues of each sequence the RMSD is an average of only it and its neighbor.

Lys281 of PEPC22 NOE cross-peaks were observed between the main chain NH to Hγ, H_δ, and H_ϵ. Cross-peaks were also observed from H_α to Hγ and to H_ϵ. Since variation in the mixing time from 50 to 200 ms gave no indication that these contacts derived from spin diffusion, it is apparent that this side chain spends much of its time in a folded conformation. Other interactions, such as Ser282 NH to Lys281 Hγ and Trp278 H_α to Lys281 Hγ are also not consistent with a fully extended chain. All the calculated structures for Lys281 showed a gauche rotation between Cγ and C_δ. This residue was also unique in that about one-half of the calculated structures showed the lysine oriented toward one side of the hydrophobic sector of the α-helix and the remainder on the other side (due to an α,β gauche rotation). In addition, the γ,δ gauche rotation was opposite, so that the two orientations were approximately mirror images. When one orientation was selected and the calculations repeated, the 50:50 split between orientations was again obtained. Long-range side chain contacts with the backbone NH and H_α protons were seen in other well-defined lysines such as Lys248 or -252. However, unlike Lys281, no contacts were observed between the Hγ, H_δ, or H_ϵ protons of Lys248 or Lys252 and the NH protons of the $n + 1$ residue at Val249 or Val253, respectively (refer to Figure 9). The extra interaction of Lys281 with the backbone NH at Ser282 apparently accounts for the 50:50 distribution of orientations of the Lys281 side chain toward opposite sides of the hydrophobic sector.

While most of the acidic amino acid side chains in both peptides were positioned near the center of the polar face, the disposition of three glutamates was interfacial. Interestingly, these three residues occupy the second position of the conserved 11-mer repeat, Glu257, Glu268, and Glu279. Glu268 is the final residue in PEPNH1 and the second residue in PEPC22. As a consequence, in both peptides the exact position of Glu268 was not well determined because of the paucity of NOE constraints near the termini (see Figure 4). The remaining two glutamates are found in the well-defined midportion of the peptide backbone. The glutamate side chains were predominently extended although some of the calculated structures contained a gauche rotation about the C_β−Cγ bonds. This gauche rotation directed the carboxyl group away from the hydrophobic face of the peptide toward the interfacial region.

Analysis of primary sequences of membrane-spanning helices suggests that aromatic amino acid side chains tend to be located near the aqueous surfaces rather than deep in the bilayer interior (Von Heijne, 1994). Similar proposals have been based on fluorescence quenching of Trp and Tyr analogs by spin-labeled phospholipids (Kachel et al., 1995). The tryptophan side chains of both CT peptides were oriented so that the indole nitrogen was positioned close to the polar/nonpolar face while the bulk of the associated ring system extended into the nonpolar face of the peptide. Studies in amphiphilic liquid crystalline systems have shown that aromatic rings are located within the hydrocarbon core of the bilayer with the polar groups directed into the interface (Radley & Tracey, 1990; Diehl & Tracey, 1975), and this arrangement apparently is followed here.

DISCUSSION

Relation of SDS-Bound Conformations to the Structure of Membrane-Bound Peptides. SDS has been commonly used as the amphiphile in the NMR determination of the structures of membrane-bound peptides (Opella et al., 1994; Henry & Sykes, 1994). SDS preserves the secondary structure of membrane binding peptides (Tanford & Reynolds, 1976). For the fd phage coat protein, compatible information for the computation of a structure was obtained from solution NMR spectral analysis of the SDS-bound protein and solid-state NMR analysis of the protein bound to phospholipid multilayers (McDonnell et al., 1993). The CD spectra of the two CT peptides of this study showed that there was a close correspondence between the conformations of these peptides when bound either to vesicles or to SDS micelles. This suggests that the NMR structures obtained from SDS micellar solution are good representations of the native membrane-bound structures.

Domain M Is One Unbroken α-Helix with an N-Terminal Hinge. An unbroken helical structure for residues 242−288 of domain M (PEP62) is suggested by the α-helical structures of the two overlapping peptides, and is supported by the findings that the α-proton chemical shifts of PEP62 lie within the range of those of the two smaller segments and that the general patterns of the NOESY spectra of PEPNH1 and PEPC22 were reflected in the NOESY spectrum of PEP62. The two CT peptides overlap at just two residues, Val267 and Glu268. The structure of the peptide backbone is quite well defined at these residues in PEPNH1 but less well defined in PEPC22. It is very unlikely that the helix would be interrupted at these two residues. This region represents

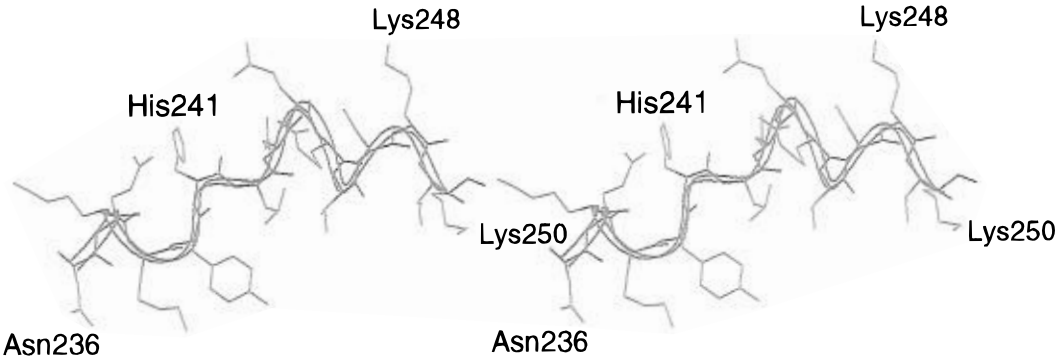

FIGURE 8: Stereo diagram showing the backbone and side chains of the hinge region of PEPNH1. The average of 10 calculated structures is represented.

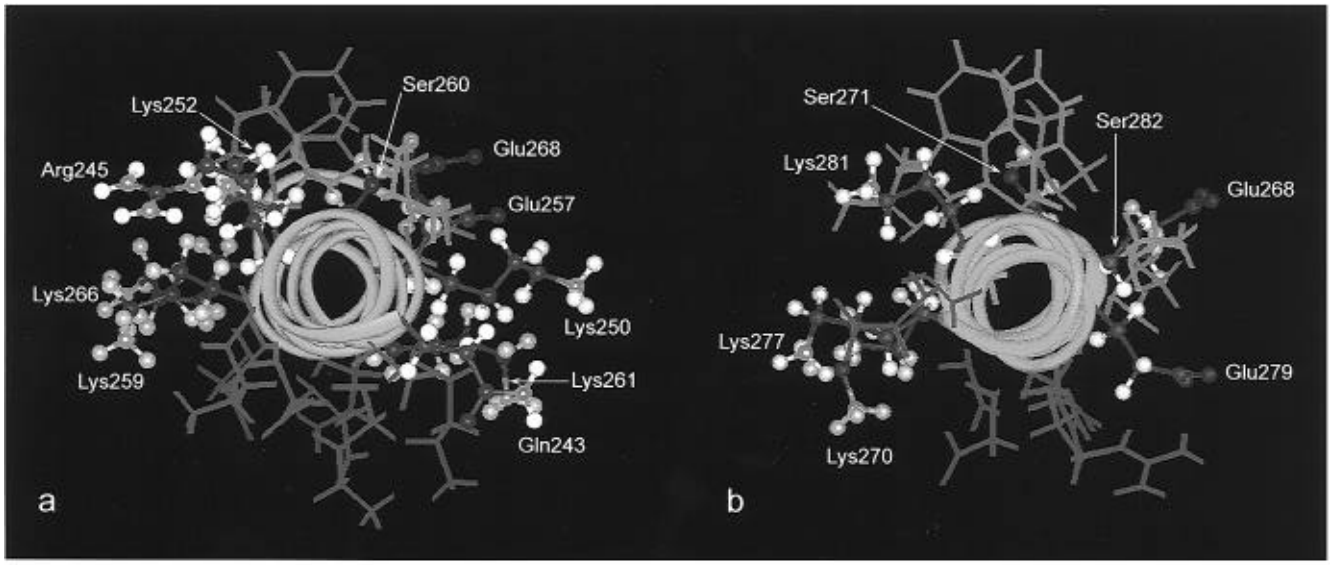

FIGURE 9: Diagrams showing the distribution of side chains about the α-helical portion of (A) PEPNH1 (residues 243−268) and (B) PEPC22 (all residues). The average distribution from 10 calculated structures is displayed: hydrophobic side chains, light green; hydrophilic side chains, magenta.

the start of the second conserved 11-mer repeat, and the first and third repeats are helical throughout the corresponding regions. The peptides studied here do not extend to the C-terminus of domain M (residue 298). A turn is predicted to occur between residues 294 and 297. This turn would connect domain M via a hinge to the C-terminal section of CT. The folding of domain M into a helix creates a very long hydrophobic face for lipid intercalation. Since CT is a homodimer (Cornell, 1989), the membrane binding surface area for the active enzyme may be as great as twice the surface area of the hydrophobic face of the 62-mer, which is ∼1000 Å^2. While examples of amphipathic helices serving to anchor proteins to membrane surfaces are emerging (Picot et al., 1995; Gilbert & Baleja, 1995; Stroud, 1995), CT is so far unique in that one very long (≥52 residue) unbroken helix mediates the interaction.

Helix-Stabilizing Factors. One of the major factors contributing to the stability of the α-helix is the hydrophobic stabilization provided by the interactions of the nonpolar face of the helix and the lipid core. Transfer of the 18 hydrophobic side chains in the sequence between Leu242 and Phe 293 from water to solvent of dielectric 2 is associated with a free energy of transfer of −54 kcal/mol based on the GES scale (Engelman et al., 1986). In addition to the unfavorable entropy changes upon binding, the hydrophobic driving force would be opposed by the stabilizing interactions of the lipid bilayer in the headgroup and acyl chain region. These interactions would have to be disrupted to allow peptide intercalation. This lipid perturbation factor might not be as significant for SDS as for the more hydrophobic lipids because of its increased solubility in water. Lipids that weaken bilayer packing promote CT−membrane binding (Cornell, 1991).

In light of the propensity for an α-helical conformation and the strong hydrophobic driving force for membrane intercalation, it is surprising that, in most cells, CT is predominently localized to a soluble rather than to a membrane fraction. Perhaps in its soluble form, domain M of CT interacts as an amphipathic α-helix with a protein surface via hydrophobic and electrostatic forces. This protein surface could be another domain of CT or located on a separate protein. The distribution between cytosolic and membrane-bound forms would then depend on competition between the phospholipid surface and the protein surface for domain M binding.

Another helix-stabilizing factor arises from the arginines and lysines that form strips of positive charge along the polar/nonpolar interface of the peptides. These positive interfaces are only present when the peptides assume helical conformations. These basic side chains would interact electrostatically with the negatively charged amphiphiles of the surface: SDS in the NMR structure; anionic phospholipids in the membrane. The requirement for an anionic surface to stabilize the α-helical structure demonstrates the

functional importance of these basic side chains. All of the basic interfacial residues are conserved among five mammalian CT clones, with the exception of Lys277. In a clone from CHO cells, Lys277 is substituted with a threonine (Sweitzer & Kent, 1994).

Several studies have suggested that ion pairing interactions between basic and acidic residues separated by three or four amino acids contribute to helix stability (Sundaralingham et al., 1985; Marqusee & Baldwin, 1987; Merutka & Stellwagen, 1991). There are 14 potential ion pairs within the α-helical regions of the two CT peptides. The distances between potential pairs of side chains were in the order of 7−10 Å. In no case was the lower limit close to the 3.5 Å separation needed to form an electrostatic link. Thus ion pairing interactions are not important for the stabilization of this helix. Similar conclusions have been drawn from structural studies of other lipid-binding amphipathic helices (Rozek et al., 1995).

Basis for Reversibility of Membrane Binding. The reversible nature of the binding of CT to a membrane is central to CT regulation. The soluble form of CT is inactive while the membrane-bound form is active. One likely contribution to the reversibility is the interruption of the hydrophobic face of the helix by serines-260, -271, and -282, which are conserved in all five mammalian CT clones. Serine falls near the center of most hydrophobic scales (Reithmeier & Deber, 1992) and is compatible with a lipidic localization since its side chain hydroxyl group can H-bond with the peptide backbone and would not project beyond the lipid headgroup region. Thus, while these three serines do not contribute to hydrophobic stabilization, neither do they interfere with it. If, however, the serines were replaced with a bulky nonpolar group, the hydrophobic binding force would be increased. Substitution of the three serines for alanine in a 33-mer peptide, corresponding to the 11-mer repeats of domain M, resulted in increased hydrophobicity and membrane partition coefficient (Johnson, 1995). Furthermore, the selectivity of this peptide for anionic lipids decreased. Therefore, these three serines may serve to limit the hydrophobic binding strength, which would facilitate dissociation from the membrane and would enhance binding selectivity.

Basis for the Selectivity for Anionic Surfaces. PEPNH1 has a net charge of +3 and PEPC22 has a net charge of −2, yet both peptides show selectivity for anionic lipids (Johnson, 1995). Obviously, factors other than the net charge of the peptide must account for the lipid binding selectivity. The most important factor is likely the segregation of the basic amino acids to the interfaces flanking the hydrophobic sector. In PEPNH1, all but two of the nine lysine or arginine residues are oriented interfacially, where they are distributed three to one side of the hydrophobic sector and four to the opposite side (Figure 9A). For one-half of the calulated structures of PEPC22, all three lysines are located at one interface while an arginine is located toward the opposite side, as shown in Figure 9. In the other calculated structures Lys281 is oriented to the same side as Arg283. Lysine-281 was unique in having dual orientations with respect to the hydrophobic sector. Arg245, Lys252, and Lys281 are found in the hydrophobic face. This arrangement is similar to that found for two arginines of the phosphatidylserine-selective membrane binding amphipathic α-helix of coagulation factor VIII (Gilbert & Baleja, 1995). In contrast to this, the acidic side chains in both peptides are disposed toward the center of the polar face (except for glutamates-257, -268, and -279 discussed below). The positioning of basic side chains in the interfacial region would determine the selectivity for anionic surfaces and, moreover, would control the degree of penetration of the helix into the hydrophobic domain of the membrane.

The amphipathic helix of CT has three acidic residues, Glu257, Glu268, and Glu279, that orient to one interface. In the SDS-bound structures these glutamates are drawn very close to the hydrophobic face. Two potential functions of these glutamates are (i) to limit the hydrophobicity of domain M, thereby facilitating release from the membrane, and (ii) to increase the selectivity for anionic surfaces. The apparent contradiction in this latter function is explained by the creation of an increased proton concentration at the anionic surface, which would result in protonation and charge neutralization of the glutamate, thus increasing the hydrophobicity of the peptide. A pH-dependent binding preference for acidic membranes of a model glutamate-containing peptide was recently described in these terms (Leenhouts et al., 1995). The pK_a values of two interfacial aspartate and glutamate residues in an apo A-I peptide were shifted 1 pH unit higher when bound to SDS as compared to DPC (Wang et al., 1996). An apolipoprotein peptide analog (18R) has reversed charge distribution compared to the normal class A amphipathic helix (Segrest et al., 1990), with positive charges in the center of the polar face and negative charges at the interfaces. Nevertheless, this peptide had ∼5-fold selectivity for anionic phospholipids (Spuhler et al., 1994). It was proposed that the acidic residues flanking the polar/nonpolar interfaces were protonated upon binding to the anionic lipid surface (Spuhler et al., 1994). The recent observation that the membrane binding and activation of CT by negatively charged lipid vesicles can be enhanced by a decrease in pH is compatible with a CT protonation event that would enhance its hydrophobicity (Arnold & Cornell, 1996). The role of the interfacial glutamates and lysines in determining the lipid selectivity of the CT peptides and the whole enzyme could be probed by substitution with uncharged or oppositely charged amino acids.

Function of the Bend near the N-Terminus of PEPNH1. A turn in the segment linking the catalytic and regulatory domains has previously been proposed (Craig et al., 1994). The NMR-derived structure reveals the presence of a well-defined bend at His241 (Figure 7). The presence of the bend is not surprising since the sequence N-terminal to the bend (Asn236 through His241) is very hydrophilic and would have a preference for the aqueous phase. In the absence of the bend, the amphipathic region C-terminal to the bend would force polar side chains of the N-terminal segment into the hydrophobic core of the membrane. In the SDS-complexed PEPNH1, the direction that this hinge segment adopts is not constrained by any domains N-terminal to it nor is it constrained by a surrounding bilayer. Because of its hydrophilicity, it probably extends into the bulk water without any bound SDS. In the NMR structure the N-terminal helix is directed into the interfacial plane of the amphipathic helix. In the holoenzyme the direction would be determined by the globular catalytic domain linked to its N-terminus.

The structure of the peptide mellitin has been determined in both the micelle-bound and vesicle-bound states, the latter using transferred NOE data (Okada et al., 1994). The C-terminal four-residue segment of mellitin was α-helical

in the micelle-bound state, whereas in the vesicle-bound state it was unstructured. As is the case of the CT PEPNH1 peptide, an ordered α-helix when bound to vesicles would have forced polar side chains into the lipid phase.

The segment linking the end of the conserved domain (Ser233) to the beginning of the amphipathic helix (at Leu242) is potentially very important to the function of CT because changes in the conformation of domain M could influence the catalytic domain via modulation of this hinge. Mutations in which CT is truncated at different sites within or in close proximity to this hinge result in very different properties for reasons that are obscure. A mutant truncated at residue 236 was constitutively active (Wang & Kent, 1995) whereas mutants truncated at residues 257, 231 (Yang et al., 1995), or 228 (Cornell et al., 1995) were relatively inactive. A chymotrypsin fragment that truncates at residue 225 was also inactive (Veitch & Cornell, 1996). Clearly this is a region of CT that will receive closer attention in future studies.

SUPPORTING INFORMATION AVAILABLE

Table 1A showing ^{1}H chemical shifts (ppm) and ΔH_α values for the CT fragment 236−268 (PEPNH1) and Table 1B showing ^{1}H chemical shifts (ppm) and ΔH_α values for the CT fragment 267−288 (PEPC22) (4 pages). Ordering information is given on any current masthead page.

REFERENCES

Arnold, R. S., & Cornell, R. B. (1996) *Biochemistry 35*, 9917−9924.

Burn, P. A. (1988) *Trends Biochem. Sci. 13*, 79−82.

Casey, P. (1995) *Science 268*, 221−225.

Chang, C. T., Wu, C.-s., & Yang, J. T. (1978) *Anal. Biochem. 91*, 13−31.

Clark-Lewis, I., Walz, A., Baggiolini, M., Scott, G., & Aebersold, R. (1991) *Biochemistry 30*, 3128−3135.

Cornell, R. B. (1989) *J. Biol. Chem. 264*, 9077−9082.

Cornell, R. B. (1991) *Biochemistry 30*, 5881−5888.

Cornell, R. B., Kalmar, G. B., Kay, R. J., Johnson, M. A., Sanghera, J. S., & Pelech, S. L. (1995) *Biochem. J. 310*, 699−708.

Craig, L., Johnson, J. E., & Cornell, R. B. (1994) *J. Biol. Chem. 269*, 3311−3317.

de Dios, A. C., Pearson, J. C., & Oldfield, E. (1993) *Science 260*, 1491−1496.

Diehl, P., & Tracey, A. S. (1975) *Can. J. Chem. 53*, 2755−2762.

Engelman, D., Steitz, T., & Goldman, A. (1986) *Annu. Rev. Biophys. Biophys. Chem. 15*, 321−353.

Gilbert, G. E., & Baleja, J. D. (1995) *Biochemistry 34*, 3022−3031.

Henry, G., & Sykes, B. (1994) *Methods Enzymol. 139*, 515−535.

Hogan, M., Zimmermann, L., Wang, J., Kuliszewski, M., Liu, J., & Post, M. (1995) *Am. J. Physiol. 267*, L25−L32.

Johnson, J. E. (1995) Identification and Characterization of a Membrane Binding Amphipathic α-Helical Domain of CTP: Phosphocholine Cytidylyltransferase, Ph.D. Thesis, Simon Fraser University.

Johnson, J. E., & Cornell, R. B. (1994) *Biochemistry 33*, 4327−4335.

Kachel, K., Asuncion-Punzalan, E., & London, E. (1995) *Biochemistry 34*, 15475−15479.

Kalmar, G. B., Kay, R. J., La Chance, A., Aebersold, R., & Cornell, R. B. (1990) *Proc. Natl. Acad. Sci. U.S.A. 87*, 6029−6033.

Kalmar, G. B., Kay, R. J., LaChance, A., & Cornell, R. B. (1994) *Biochim. Biophys. Acta 1219*, 328−334.

Le, H. B., Pearson, J. G., de Dios, A. C., & Oldfield, E. (1995) *J. Am. Chem. Soc. 117*, 3800−3807.

Leenhouts, J. M., van den Wijngaard, P. W. J., de Kroon, A. I. P. M., & de Kruijff, B. (1995) *FEBS Lett. 370*, 189−192.

Marqusee, S., & Baldwin, R. L. (1987) *Proc. Natl. Acad. Sci. USA 84*, 8898−8902.

McDonnell, P., Shon, K., Kim, Y., & Opella, S. J. (1993) *J. Mol. Biol. 233*, 447.

Merutka, G., & Stellwagen, E. (1991) *Biochemistry 30*, 1591−1594.

Okada, A., Wakamatsu, K., Miyazawa, T., & Higashijima, T. (1994) *Biochemistry 33*, 9438−9446.

Opella, S. J., Kim, Y., & McDonnell, P. (1994) *Methods Enzymol. 139*, 536−560.

Picot, D., Loll, P., & Garavite, R. M. (1995) *Nature 367*, 243−249.

Piotto, M., Saudek, V., & Sklenar, V. (1992) *J. Biomol. NMR 2*, 661−665.

Radley, K., & Tracey, A. S. (1990) *Mol. Cryst. Liq. Cryst. 182B*, 177−184.

Rance, M., Sorensen, O. W., Bodenhausen, G., Wagner, G., Ernst, R. R., & Wüthrich, K. (1983) *Biochem. Biophys. Res. Commun. 117*, 479−485.

Reithmeier, R., & Deber, C. (1992) in *The Structure of Biological Membranes* (Yeagle, P., Ed.) pp 337−393, CRC Press, Boca Raton, FL.

Rizo, J., Blanco, F., Kobe, B., Bruch, M., & Gierasch, L. (1993) *Biochemistry 32*, 4881−4894.

Rozek, A., Buchko, G., & Cushley, R. J. (1995) *Biochemistry 34*, 7401−7408.

Rutherford, M. S., Rock, C. O., Jenkins, N. A., Gilbert, D. J., Tessner, T. G., Copeland, N. G., & Jackowski, S. (1993) *Genomics 18*, 698−701.

Segrest, J. P., de Loof, H., Dohlman, J. G., Brouillette, C. G., & Anantharamaiah, G. M. (1990) *Proteins 8*, 103−117.

Sklenar, V., Piotto, M., Leppik, R., & Saudek, V. (1993) *J. Magn. Reson., Ser. A 102*, 241−245.

Spuhler, P., Anantharamaiah, G. M., Segrest, J. P., & Seelig, J. (1994) *J. Biol. Chem. 269*, 23904−23910.

Stroud, R. (1995) *Curr. Opin. Struct. Biol. 5*, 514−520.

Sundaralingham, M., Drendel, W., & Greaser, M. (1985) *Proc. Natl. Acad. Sci. USA 82*, 7944−7947.

Sutton, R. B., Davietov, B. A., Berghuis, A. M., Sudhof, T. C., & Sprang, T. R. (1995) *Cell 80*, 929−938.

Sweitzer, T., & Kent, C. (1994) *Arch. Biochem. Biophys. 311*, 107−116.

Tanford, C., & Reynolds, J. (1976) *Biochim. Biophys. Acta 457*, 133−170.

Timm, D., Salim, K., Gout, I., Guruprased, L., Waterfield, M., & Blundell, T. (1994) *Nat. Struct. Biol. 1*, 782−788.

Tronchere, H., Record, M., Terce, F., & Chap, H. (1994) *Biochim. Biophys. Acta 1212*, 137−151.

Veitch, D., & Cornell, R. B. (1996) *Biochemistry* (in press).

von Heijne, G. (1994) *Annu. Rev. Biophys. Biomol. Struct. 23*, 167−192.

Wang, G., Treleaven, W. D., & Cushley, R. J. (1996) *Biochim. Biophys. Acta 1301*, 174−184.

Wang, Y., & Kent, C. (1995) *J. Biol. Chem. 270*, 18948−18952.

Wang, Y., Sweitzer, T., Weinhold, P. A., & Kent, C. (1993) *J. Biol. Chem. 268*, 5899−5904.

Wang, Y., MacDonald, J., & Kent, C. (1995) *J. Biol. Chem. 270*, 354−360.

Wishart, D. S., & Sykes, B. D. (1991) *J. Mol. Biol. 222*, 311−333.

Wishart, D. S., Sykes, B. D., & Richards, F. M. (1992) *Biochemistry 31*, 1647−1651.

Wüthrich, K (1986) *NMR of Proteins and Nucleic Acids*, John Wiley & Sons, New York. Yang, W., Boggs, K. P., & Jackowski, S. (1995) *J. Biol. Chem. 270*, 23951−23957.

Zhang, G., Zazaniete, M. G., Blumberg, P. M., & Hurley, J. H. (1995) *Cell 81*, 917−924.

BI960821+